Proc. Natl. Acad. Sci. USA
Vol. 86, pp. 3544–3548, May 1989
Biochemistry

Cadmium resistance from *Staphylococcus aureus* plasmid pI258 *cadA* gene results from a cadmium-efflux ATPase

(E_1E_2-type ATPase/heavy-metal plasmid resistance)

GIUSEPPINA NUCIFORA, LIEN CHU, TAPAN K. MISRA, AND SIMON SILVER

Department of Microbiology and Immunology, University of Illinois College of Medicine, Chicago, IL 60680

Communicated by Emanuel Margoliash, January 30, 1989

ABSTRACT **Cadmium resistance specified by the *cadA* determinant of *Staphylococcus aureus* plasmid pI258 results from the functioning of a cadmium-efflux system. In the nucleotide sequence of the DNA fragment containing the *cadA* determinant, two open reading frames were identified. The larger one, corresponding to a predicted polypeptide of 727 amino acid residues, is necessary and sufficient for expression of cadmium resistance. Comparison of the CadA amino acid sequence with known protein sequences suggested that CadA is a member of the E_1E_2 cation-translocating ATPases, similar to the K^+-uptake ATPases of Gram-positive and Gram-negative bacteria. The sequence homology is lower but significant with other E_1E_2-type ATPases, including the H^+-efflux ATPases of eukaryotic microbes and the Ca^{2+}- and Na^+/K^+-ATPases of animals. A frame-shift mutation in the middle of the gene destroys the Cd^{2+}-resistance phenotype. A detailed model for the putative CadA ATPase based on homologies to other E_1E_2 ATPases is presented and discussed.**

Resistance to Cd^{2+} is widespread in *Staphylococcus aureus* (1). There are two separate Cd^{2+}-resistance determinants, *cadA* and *cadB*, located on plasmids (2). The *cadB* gene product may protect the cell by binding Cd^{2+} (3). The resistance function coded by the *cadA* determinant results from decreased intracellular accumulation of Cd^{2+} (4), mediated by an energy-dependent efflux mechanism (5).

In *S. aureus*, Cd^{2+} enters the cell by the Mn^{2+} active transport system (4, 6), but cells that have the *cadA* gene have lower net accumulation. The CadA-efflux system is sensitive to metabolic inhibitors such as uncouplers but is not affected by agents that eliminate the membrane potential (5). Therefore, it was proposed (5) that the *cadA* product is an electroneutral antiporter that ejects one Cd^{2+} while accumulating two protons.

We have cloned the *cadA* determinant from *S. aureus* plasmid pI258 and expressed it in *Bacillus subtilis*. The DNA sequence was determined.* It consists of a single open reading frame (ORF) very likely coding for an E_1E_2 cation-translocating ATPase.

METHODS

Bacterial Strains. For cloning of the *cadA* determinant of plasmid pI258 into the vector pSK265 (7), *B. subtilis* strain BD224 (8) (*trpC2 recE4 thr-5*) (BGSC 1 A46, *Bacillus* Genetic Stock Center, Columbus, OH) was used. The cells were grown in tryptone broth (8 g of Difco Bacto tryptone and 5 g of NaCl per liter) supplemented with threonine and tryptophan (50 μg/ml each). When necessary for selection, chloramphenicol (5 μg/ml) was added to liquid medium or to the tryptone broth agar plates.

Uptake Assays. The cells were grown to a density of 100 Klett turbidity units (no. 54 Kodak Wratten filter) at 37°C with shaking, harvested by centrifugation at 6800 × *g* for 7 min, and suspended in medium at a density of 25 mg (dry weight)/ml. The final cell density in transport assays was 0.5 mg (dry weight)/ml. Transport assays were at 37°C in broth with aeration by shaking. Samples were filtered through 0.45-μm pore-diameter filters (Bio-Rad) and rinsed twice with 5 ml of NaCl solution (9 g/liter). Radioactive samples were assayed in a liquid scintillation spectrometer (Packard Instrument).[1]

DNA Cloning and Sequencing. For construction of plasmids and phage M13 derivatives containing the *cadA* determinant, a derivative of pRAL1 (1, 9) was used. The 3.5-kilobase (kb) *Bgl* II–*Xba* I DNA fragment, previously identified by Novick *et al.* (2) as containing the *cadA* Cd^{2+}-resistance determinant, was cloned into phage mTM010 (10) in both orientations. Nested deletions for sequencing were made by using BAL-31 exonuclease (10). The 3.5-kb fragment was also cloned into vector pSK265 (7) (for expression in *B. subtilis*). Two recombinant plasmids, pGN114 and pGN115, containing the entire 3.5-kb DNA fragment in opposite orientations, were generated.

Plasmids pGN116-1 and pGN116-2 [containing the intact larger ORF (ORF2, *cadA*) cloned in both orientations] were obtained by ligating into the vector plasmid pSK265 a DNA fragment generated by BAL-31 deletion and lacking the first 920 base pairs (bp) of the *Bgl* II–*Xba* I fragment shown in Fig. 1. This fragment was introduced also in pGEM-3Zf(+) (Promega Biotec) under control of the T7 phage transcriptional promoter to generate pGN118 [for the expression of the CadA protein in *Escherichia coli* strain BL21 (11)], containing the T7 RNA polymerase under the control of the inducible *lacUV5* promoter.

Mutant plasmid pGN117, containing the entire 3.5-kb DNA fragment with a frame-shift mutation in the *cadA* gene, was obtained by Klenow DNA polymerase conversion of the protruding ends generated by *Xho* I (see Fig. 1) digestion of pGN114 to blunt ends.

Membrane Preparation, Solubilization and Reconstitution of Proteoliposomes, and Transport Assays. The procedure of Ambudkar *et al.* (12), slightly modified, was used for the preparation of bacterial membranes. Membranes and proteoliposomes were suspended in 20 mM Mops, pH 7/200 mM KCl and used immediately. For transport assays, membrane vesicles or proteoliposomes were mixed with $^{109}Cd^{2+}$. After 3–5 min at 0°C, the reaction was initiated by the addition of 5 mM ATP and 5 mM Mg^{2+}. Aliquots (0.1 ml) were filtered on Millipore filters (pore size, 0.22 μm) and washed with assay buffer containing $MgSO_4$. The radioactive samples were assayed in a scintillation counter.

The publication costs of this article were defrayed in part by page charge payment. This article must therefore be hereby marked "*advertisement*" in accordance with 18 U.S.C. §1734 solely to indicate this fact.

Abbreviation: ORF, open reading frame.

*The sequence reported in this paper is being deposited in the EMBL/GenBank data base (accession no. J04551).

Labeling of Proteins with [^{32}P]ATP. Cell membranes were incubated in 50 mM Mops (pH 7.2)/5% (vol/vol) glycerol/5 mM $MgCl_2$ at 4°C; 10 μM [^{32}P]ATP (10 μCi; 1 μCi = 37 kBq) was added, and incubation was continued at 4°C for 15 sec. After addition of cold 10% (wt/vol) trichloroacetic acid/1 mM phosphate and centrifugation, the precipitate was washed with cold H_2O, suspended in loading buffer, and resolved by electrophoresis on an acidic lithium dodecyl sulfate/polyacrylamide gel (13, 14).

RESULTS

Nucleotide Sequence of the *cadA* Determinant. Fig. 1 shows the nucleotide sequence of the 3535 bp containing the *cadA* determinant and the amino acid translation of the two major ORFs. The sequence starts ≈200 bp from the *Xba* I site of the physical map of plasmid pI258 (1, 2) and ends at the *Bgl* II site. Of the two major ORFs identified, the first one starts at position 704, after a segment of DNA containing direct and inverted repeats (indicated by arrows a through h in Fig. 1) and ends at nucleotide 1072. The resulting predicted peptide contains 122 amino acids. From deletion experiments (see below), the first 920 bp containing the repeats and coding for part of the short polypeptide appear not necessary for resistance to Cd^{2+}. At position 1065, a second and longer ORF starts that overlaps 8 bp with the previous one. Upstream of the ATG start codon there are a reasonably good

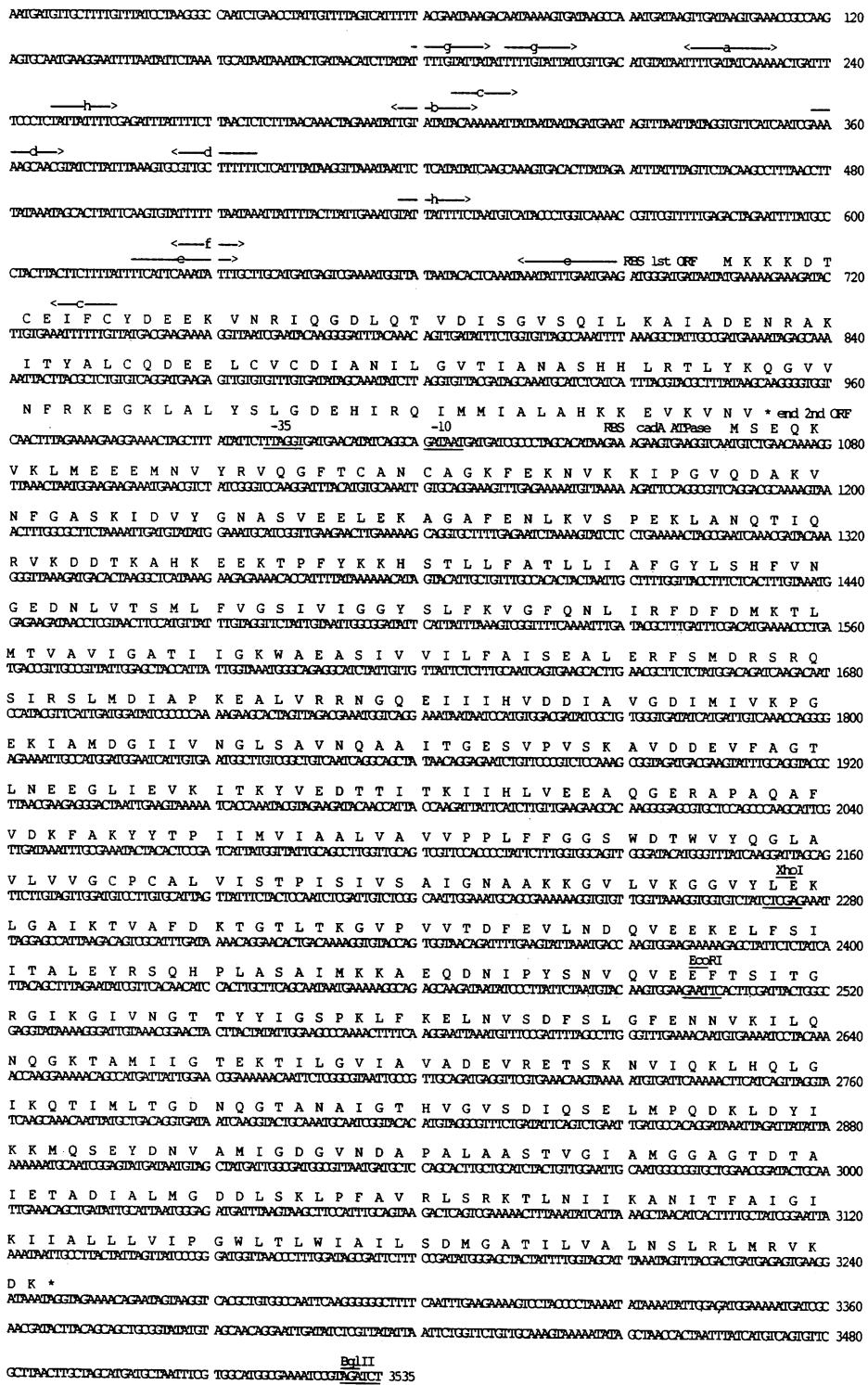

FIG. 1. Nucleotide sequence of the 3535 bp of the *cadA* determinant from plasmid pI258. The strand equivalent to the mRNA is shown. Ribosome binding site (RBS), predicted polypeptides, and three restriction nuclease sites (*Xho* I, *Eco* RI, and *Bgl* II) used for cloning or mutations are indicated. Inverted repeat sequences a through f and direct repeats g and h of 10 bp or longer in the region from base pair 219 to 737 are shown by labeled arrows.

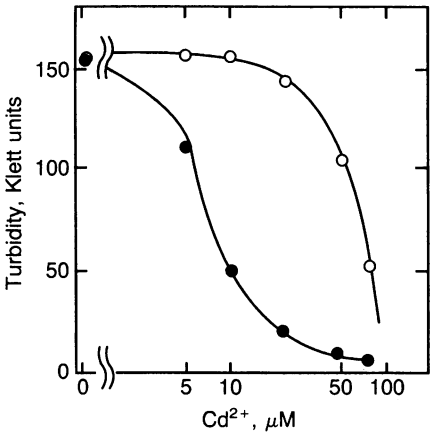

FIG. 2. Cd^{2+} resistance of *B. subtilis* BD224 strains containing the recombinant plasmid pGN114 (○) or vector plasmid pSK265 (●). Overnight cultures were diluted 1:100 in tryptone broth containing Cd^{2+}. Culture turbidities were measured after 7 hr of growth.

potential ribosomal binding site and a transcriptional initiation signal (marked on Fig. 1). This ORF continues for 2184 bp, corresponding to a predicted 727-amino acid polypeptide.

Alignment of the 200 bp flanking the *Bgl* II site with the left end of the IS*427* insertion sequence element of plasmid pI524 (also from *S. aureus*) sequenced by Barberis-Maino *et al.* (15) showed a perfect match of the 134 terminal bp (not shown).

Cd^{2+} Resistance Is Determined by a Single ORF. Fig. 2 shows the effect of increasing concentration of Cd^{2+} on the growth of *B. subtilis* cells carrying plasmids pSK265 (sensitive) or pGN114 (resistant; the entire 3.5-kb *Bgl* II–*Xba* I fragment). The cells with the recombinant plasmid grew in the presence of 10 times the concentration of Cd^{2+} that the sensitive cells would tolerate. Similar results were obtained with cells containing plasmid pGN115, where the insert had been cloned in opposite orientation (not shown).

In cation transport experiments, cells containing pSK265 or pGN114 took up equivalent amounts of $^{54}Mn^{2+}$ over the 5-min time course of an uptake experiment. However, the sensitive cells took up 2–4 times more $^{109}Cd^{2+}$ than the resistant cells (Fig. 3). Note that the uptake of Cd^{2+} was 20 times more in Fig. 3 than that of Mn^{2+}, similar to the ratio in earlier studies (16). The roles of the two major ORFs in the cloned fragment were investigated by repeating growth and $^{109}Cd^{2+}$ uptake experiments with cells transformed by plasmids pGN116-1 and pGN116-2 (containing only the larger ORF cloned in opposite orientations in the vector) and by plasmid pGN117 (where a framshift mutation had been introduced in the large ORF 35 bp upstream of the codon for the aspartate residue believed to be critical to the activity of E_1E_2 ATPases; see *Discussion* below). In this mutant, the first ORF had therefore been left intact. The results indicate that the protein encoded by the large ORF is necessary and sufficient for Cd^{2+} resistance (data not shown) and for

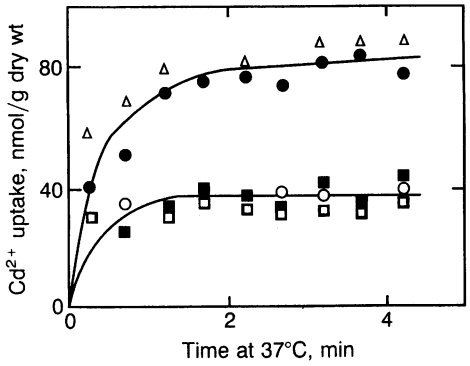

FIG. 4. Uptake of $^{109}Cd^{2+}$ by *B. subtilis* cells containing plasmid vector pSK265 (●), recombinant plasmid pGN114 (○), the *cadA* large ORF cloned in both orientations in pSK265 to form pGN116-1 (□) and pGN116-2 (■), and the mutant pGN117 (△) in which a frame-shift mutation has been introduced in *cadA* by *Xho* I digestion blunt-end conversion with Klenow DNA polymerase, and ligation.

reduced Cd^{2+} uptake (Fig. 4). Comparable results with pGN116-1 and pGN116-2 indicate that *cadA* is expressed by using its own promoter.

Analysis of the Predicted Polypeptides. The amino acid sequences predicted from the two major ORFs were checked against protein libraries for related proteins by using a polypeptide alignment program (17). No significant homology was found for the smaller protein. However, the 727-amino acid polypeptide showed significant matches with bacterial and eukaryotic E_1E_2 cation-transport ATPases (Table 1). Fig. 5 shows the alignment of the 727-amino acid CadA polypeptide with the K^+-ATPase from *Strep. faecalis* (17), which is the closest to the CadA polypeptides of currently published E_1E_2-type ATPase sequences.

***In Vitro* Measurements of ATPase Activity, Protein Phosphorylation, and Cd^{2+} Transport.** Attempts were made to overproduce the 727-amino acid protein (11), to measure ATPase activity of the protein *in vitro*, to measure uptake of $^{109}Cd^{2+}$ in everted membrane vesicles of *B. subtilis* and in proteoliposomes (12), and to measure a large polypeptide that could be labeled with [^{32}P]ATP (13). This series of experiments has not been successful. When the T7 RNA polymerase was induced for the expression of the *cadA* gene under the control of the phage T7 promoter (11), cell growth stopped abruptly, and the surviving cells contained plasmids where the insert was partially or completely deleted.

DISCUSSION

The sequence homology between the *cadA* gene product and E_1E_2-type ATPases suggests that Cd^{2+} resistance is mediated by a Cd^{2+}-translocating ATPase. This is consistent with the physiological results of Tynecka *et al.* (5), who demonstrated that Cd^{2+} resistance results from energy-dependent Cd^{2+}

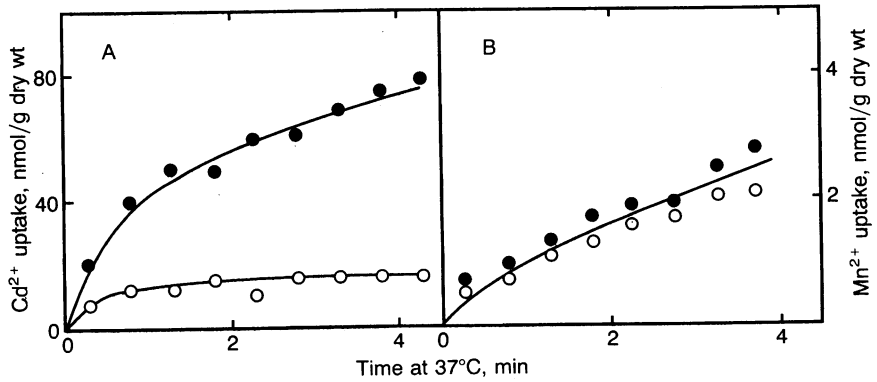

FIG. 3. Uptake of $^{109}Cd^{2+}$ (*A*) and of $^{54}Mn^{2+}$ (*B*) by sensitive *B. subtilis* cells containing plasmid pSK265 (●) and by resistant cells containing plasmid pGN114 (○). The cells were prepared as described in the text and incubated for 2 min at 37°C; 20 μM $^{109}Cd^{2+}$ or $^{54}Mn^{2+}$ was added. Samples [0.25 mg dry weight (wt)] were filtered and washed as indicated.

Table 1. Comparison of the Cd^{2+}-ATPase sequence with other cation-translocating ATPases

ATPase source	Cation specificity	Length, aa	FASTP score	% identities (over aa range indicated)	
S. aureus	Cd^{2+}	727	3381	100	(727)
Strep. faecalis	K^+	583	703	29.8	(543)
E. coli KdpB	K^+	682	462	26.2	(577)
Sac. cerevisiae	H^+	918	179	33.1	(148)
Neurospora	H^+	920	170	29.6	(189)
Human α chain	Na^+/K^+	1023	159	35.6	(90)
Rabbit muscle	Ca^{2+}	1001	133	37.9	(95)
(*E. coli* Hg^{2+} reductase)	Hg^{2+}	561	99	32.8	(58)

Results are from a search (January 22, 1989) of the European Molecular Biology Organization library of protein sequences for polypeptides homologous to CadA using the FASTP alignment algorithm (16). The closest match found was to the *Streptococcus faecalis* K^+-ATPase sequence (18). The FASTP score (17) is given in arbitrary units after optimization allowing gaps; the percent amino acid (aa) identities and the lengths of the homologous regions from the FASTP matching are shown. Results from only one of the seven current Na^+/K^+-ATPase sequences, one of the current two sarcoplasmic reticulum Ca^{2+}-ATPase sequences, and one of the five current mercuric reductase sequences are shown. The mercuric reductases are not ATPases but scored with a significant homology for the N-terminal region (see text). *Sac., Saccharomyces.*

efflux. The protein predicted by the DNA sequence shows 26–30% amino acid identities over stretches of >500 residues with the K^+-uptake ATPases of *Strep. faecalis* and *E. coli* (Table 1).

At its amino-terminal end, the putative Cd^{2+}-ATPase shares significant homology (10 SDs from the mean score for

FIG. 5. Alignment of the putative *cadA* amino acid sequence versus the K^+-ATPase from *Strep. faecalis*. Dashes indicate gaps introduced to optimize alignment, semicolons indicate identities, and dots indicate conservative amino acid replacements. The marked proline (*) and aspartate (PO_4) residues are considered in the *Discussion*.

8702 polypeptides in the current library) to mercuric reductase and to the periplasmic mercury-binding protein of the mercury-resistance operons (Table 1 and Fig. 6). The region includes conserved paired cysteine residues (Cys-23 and Cys-26 in the CadA protein). The occurrence of such paired cysteine residues has become a recurring motif in soft metal-binding regions, and they are hypothesized to play a role in the initial binding of the heavy-metal ion because of the strong affinity of their sulfhydryl groups for the heavy-metal ions (20, 21). In several E_1E_2 ATPases, the amino-terminal part of the enzyme has been postulated to provide the recognition and the initial binding site for the cation to be transported (22, 23). The models are based on analysis of enzyme functions (recognition and binding of the cation, transduction, phosphorylation, and ATP binding) after limited tryptic digestion. The E_1E_2 ATPases are primarily cytoplasmic globules formed by at least four interactive domains, connected by a narrow stalk to the hydrophobic membrane-anchoring segment of the enzyme (24–26). Transmembrane hairpins are postulated to form a channel through which the cations are transported (22, 26, 27).

There is little homology in general between eukaryotic and prokaryotic E_1E_2 ATPases in the transmembrane hairpins, beyond their positions and general hydrophobicity. The location of these hydrophobic sequences, defined by a high density of charged residues on either side of a hydrophobic segment of ≈20 amino acid residues, and their occurrence in closely positioned pairs suggest very similar overall structures for the enzymes.

The first transmembrane hairpin segment of the putative Cd^{2+} ATPase is predicted to occur between residues 106 and 148. The transmembrane segment occurs after a highly hydrophilic stretch (residues 86 through 105) and separates the amino-terminal region of the protein (concerned with the initial binding of the cation to be transported) from the transduction domain, whose primary function is the delivery of the cation to the transmembrane channel for outward translocation. The transduction domain consists of ≈180 residues in the CadA protein. It is predicted to be mostly in α-helical conformation and is highly hydrophilic (with a net negative charge provided by an excess of nine glutamate and aspartate residues). Fig. 6 shows a comparison of a relatively conserved (central) section of the putative transduction domain of the Cd^{2+}-ATPase with the corresponding regions of other E_1E_2 ATPases. The homology occurs over a stretch of about 50 residues, and it includes several conserved aspartate, glutamate, and glycine residues.

In the putative Cd^{2+}-ATPase, a second transmembrane hairpin segment is predicted next, with the second half of the hairpin containing a crucial proline residue. This proline (Pro-372, Fig. 5), is located in all E_1E_2 ATPases 43 residues before the aspartate residue (Asp-415, Fig. 5) that is phosphorylated in E_1E_2 ATPases. The position of the second transmembrane hairpin as well as the location of the proline next to the junction between transmembrane and cytoplasmic regions are in agreement with the structural model developed for other E_1E_2 ATPases (22, 24, 26, 28). Asp-415 in the CadA protein is the first of a string of 7 amino acids [Asp-Lys-Thr-Gly-Thr-Leu (or Ile)-Thr] that are conserved in E_1E_2 ATPases (from different species and with different cation-transport specificities; Fig. 6*C*) and are flanked by conservative replacements. By analogy to other E_1E_2 ATPases, Asp-415 of the CadA protein should be the aspartate residue that undergoes phosphorylation (23, 28).

The next and most extended region of homology and conservative replacements between the CadA protein and other E_1E_2 ATPases starts around residue 600 and continues for approximately 50 residues. This region is centered around two aspartate residues (Asp-620 and Asp-624 in the *cadA* gene product; Fig. 6*D*). By comparing the sequences in

A Hypothesized cation binding N-terminal region

```
                          * **  *        *  **
Cd2+ ATPase S. aureus      18 VQGFTCANCAGKFEKNVKKIPGV 40
Mercuric reductase E. coli  6 ITGMTCDSCAVHVKDALEKVPGV 28
Periplasmic Hg2+-BP E. coli 28 VPGMTCAACPITVKKALSKVEGV 50
```

B Transduction domain

```
                              **      *    *              ****
Cd2+ ATPase S. aureus     229 IHVDDIAVGDIMIVKPGEKIAMDGIIVNGL   SAVNQAAITGESVPVSKAVDDEVF 282
K+ ATPase E. coli         121 VPADQLRKGDIVLVEAGDIIPCDGEVIEGG   ASVDESAITGESAPVIRESGGDFA 174
K+ ATPase S. faecalis      96 VSLKEVHEGDRLIVRAGDKMPTDGTIDKGH   TIVDESAVTGESKGVKKQVGDSVI 149
H+ ATPase yeast           191 IPANEVVPGDILQLEDGTVIPTDGRIVTEDC FLQIDQSAITGESLAVDKHYGDQTF 246
H+ ATPase Neurospora      191 IEAPEVVPGDILQVEEGTIIPADGRIVTDDA FLQVDQSALTGESLAVDKHKGDQVF 246
Na+/K+ ATPase human       180 INAEEVVVGDLVEVKGGDRIPADLRIISAN   GCKVDNSSLTGESEPQTRSPDFTNE 234
Na+/K+ ATPase eel         180 INAEQVVVGDLVEVKGGDRIPADLRIISAC   SCKVDNSSLTGESEPQSRSPEYSSE 234
Ca2+ ATPase rabbit        140 IKARDIVPGDIVEVAVGDKVPADIRILSIKSTTLRVDQSILTGESVSVIKHTEPVPD 196
```

C Phosphoryl-aspartate region

```
                                  PO4
                              *   *****  *
Cd2+ ATPase S. aureus     404 EKLGAIKTVAFDKTGTLTKG 423
K+ ATPase E. coli         296 EAAGDVDVLLLDKTGTITLG 315
K+ ATPase S. faecalis     268 EQANDLDVIMLDKTGTLTQG 287
H+ ATPase yeast           367 ESLAGVEILCSDKTGTLTKN 386
H+ ATPase Neurospora      367 ESLAGVEILCSDKTGTLTKN 386
Na+/K+ ATPase human       365 ETLGSTSTICSDKTGTLTQN 384
Na+/K+ ATPase electric eel 365 ETLGSTSTICSDKTGTLTQN 384
Ca2+ ATPase rabbit        340 ETLGCTSVICSDKTGTLTTN 359
```

D Hinge region and end of ATP-binding domain

```
                              *  *                *** ** * *       *
Cd2+ ATPase S. aureus     598 PQDKLDYIKKMQSEYDNVAMIGDGVNDAPALAASTVGIAMGGAGTDTA 645
K+ ATPase E. coli         496 PEAKLALIRQYQAEGRLVAMTGDGTNDAPALAQADVAVAM NSGTQAA 542
K+ ATPase S. faecalis     455 PDDKEAIVQRYLDQGKKVIMVGDGINDAPSLARATIGMAI GAGTDIA 501
H+ ATPase yeast           612 PQHKYRVVEILQNRGYLVAMTGDGVNDAPSLKKADTGIAVEGA TDAR 658
H+ ATPase Neurospora      612 PQHKYNVVEILQQRGYLVAMTGDGVNDAPSLKKADTGIAVEGS SDAA 658
Na+/K+ ATPase human       695 PQQKLIIVEGCQRQGAIVAVTGDGVNDSPALKKADIGVAMGIAGSDVS 742
Na+/K+ ATPase electric eel 694 PQQKLIIVEGCQRQGAIVAVTGDGVNDSPALKKADIGVAMGIAGSDVS 741
Ca2+ ATPase rabbit        681 PSHKSKIVEYLQSYDEITAMTGDGVNDAPALKKAEIGIAM GSGTAVA 727
```

FIG. 6. Conserved sequences in eukaryotic and bacterial E_1E_2-type ATPases. Asterisks indicate identical residues in all sequences shown. (*A*) Putative cation binding N-terminal region is compared to the soft-metal-binding region of mercury-binding proteins. (*B*, *C*, and *D*) Three putative functional domains of the cation-translocating ATPases. PO_4 indicates the aspartate that undergoes phosphorylation. The primary references for the sequences shown can be found in a recent short review (19).

this region, a consensus can be extrapolated: Val-Ala-Met-Thr-Gly-Asp-Gly-Val-Asn-Asp-Ala-Pro-Ala-Leu. This region is believed to include the end of the nucleotide-binding domain (22) and extends into the next transmembrane stretch. In all of the E_1E_2 ATPases (including the postulated Cd^{2+}-ATPase), the ATPase region constitutes a single intracellular domain of 250–400 amino acids, uninterrupted by transmembrane segments.

Finally, after the last putative transmembrane hairpin, predicted to be between residues 624 and 707, the CadA molecule ends with Lys-727. The carboxyl-terminal region is considerably longer in eukaryotic E_1E_2 ATPases, where it often includes two additional transmembrane segments (23, 24, 26).

Despite different cellular origins and different specificities of cation transport and orientation, the bacterial and eukaryotic ATPases are related in function and have homologies in the regions (Fig. 6) that may correspond to the common properties of the proteins essential for their activity as primary cation pumps.

It often has been speculated that sequence similarities for E_1E_2 cation-translocating ATPases must be a consequence of a common ancestry. It is attractive to hypothesize that the proteins underwent modifications evolving the capability to transport different cations inwardly and outwardly through different membranes according to the needs for the survival of the cell, including the elimination of toxic cations.

We thank M. Walderhaug and W. Epstein for useful discussions, A. Lynn and B. P. Rosen for help with ATPase and transport assays, R. A. Laddaga for plasmid pRAL3A, S. A. Kahn for plasmid pSK265, and F. W. Studier for *E. coli* stain BL21. This work was supported by Grant DMB-86-0481 from the National Science Foundation.

1. Witte, W., Green, L., Misra, T. K. & Silver, S. (1986) *Antimicrob. Agents Chemother.* **29**, 663–669.
2. Novick, R. P., Murphy, E., Gryczan, T. J., Baron, E. & Edelman, I. (1979) *Plasmid* **2**, 109–129.
3. Perry, R. D. & Silver, S. (1982) *J. Bacteriol.* **150**, 973–976.
4. Weiss, A. A., Silver, S. & Kinscherf, T. G. (1978) *Antimicrob. Agents Chemother.* **14**, 856–865.
5. Tynecka, Z., Gos, Z. & Zajac, J (1981) *J. Bacteriol.* **147**, 313–319.
6. Tynecka, Z., Gos, Z. & Zajac, J. (1981) *J. Bacteriol.* **147**, 305–312.
7. Jones, C. L. & Khan, S. A. (1986) *J. Bacteriol.* **166**, 29–33.
8. Dubnau, D., Davidoff-Abelson, R., Scher, B. & Cirigliano, C. (1973) *J. Bacteriol.* **114**, 273–286.
9. Laddaga, R. A., Chu, L., Misra, T. K. & Silver, S. (1987) *Proc. Natl. Acad. Sci. USA* **84**, 5106–5110.
10. Misra, T. K. (1987) *Methods Enzymol.* **155**, 119–139.
11. Studier, F. W. & Moffatt, B. A. (1986) *J. Mol. Biol.* **189**, 113–130.
12. Ambudkar, S., Lynn, A. R., Maloney, P. C. & Rosen, B. P. (1986) *J. Biol. Chem.* **261**, 15596–15600.
13. Hugentobler, G., Heid, I. & Solioz, M. (1983) *J. Biol. Chem.* **258**, 7611–7617.
14. Fairbanks, G. & Avruch, J. (1972) *J. Supramol. Struct.* **1**, 66–75.
15. Barberis-Maino, L., Berger-Bächi, B., Weber, H., Beck, W. D. & Kayser, F. H. (1987) *Gene* **59**, 107–113.
16. Laddaga, R. A., Bessen, R. & Silver, S. (1985) *J. Bacteriol.* **162**, 1106–1110.
17. Lipman, D. J. & Pearson, W. R. (1985) *Science* **227**, 1435–1441.
18. Solioz, M., Mathews, S. & Fürst, P. (1987) *J. Biol. Chem.* **262**, 7358–7362.
19. Silver, S., Nucifora, G., Chu, L. & Misra, T. K. (1989) *Trends Biochem. Sci.* **14**, 76–80.
20. Silver, S. & Misra, T. K. (1988) *Annu. Rev. Microbiol.* **42**, 717–743.
21. Brown, N. L. (1985) *Trends Biochem. Sci.* **10**, 400–403.
22. Brandl, C. J., Green, N. M., Korczak, B. & MacLennan, D. H. (1986) *Cell* **44**, 597–607.
23. Shull, G. E., Schwartz, A. & Lingrel, J. B. (1985) *Nature (London)* **316**, 691–695.
24. MacLennan, D. H., Brandl, C. J., Korczak, B. & Green, N. M. (1985) *Nature (London)* **316**, 696–700.
25. Addison, R. & Scarborough, G. A. (1982) *J. Biol. Chem.* **257**, 10421–10426.
26. Addison, R. (1986) *J. Biol. Chem.* **261**, 14896–14901.
27. Brandl, C. J. & Deber, C. M. (1986) *Proc. Natl. Acad. Sci. USA* **83**, 917–921.
28. Hesse, J. E., Wieczoreck, L., Altendorf, K., Reicin, A. S., Dorus, E. & Epstein, W. (1984) *Proc. Natl. Acad. Sci. USA* **81**, 4746–4750.